

3D Monte-Carlo Device Simulations Using an Effective Quantum Potential Including Electron-Electron Interactions

CLEMENS HEITZINGER, CHRISTIAN RINGHOFER
Department of Mathematics, Arizona State University, Tempe, AZ 85287, USA
Clemens.Heitzinger@asu.edu

SHAIKH AHMED, DRAGICA VASILESKA
Department of Electrical Engineering, Arizona State University, Tempe, AZ 85287, USA

Abstract. Effective quantum potentials describe the physics of quantum-mechanical electron transport in semiconductors more than the classical Coulomb potential. An effective quantum potential was derived previously for the interaction of an electron with a barrier for use in particle-based Monte Carlo semiconductor device simulators. The method is based on a perturbation theory around thermodynamic equilibrium and leads to an effective potential scheme in which the size of the electron depends upon its energy and which is parameter-free. Here we extend the method to electron-electron interactions and show how the effective quantum potential can be evaluated efficiently in the context of many-body problems. The effective quantum potential was used in a three-dimensional Monte-Carlo device simulator for calculating the electron-electron and electron-barrier interactions. Simulation results for an SOI transistor are presented and illustrate how including the momentum of the electrons changes the result.

Keywords: Monte-Carlo simulation, effective quantum potential, electron-electron interactions.

1. Introduction

As device sizes decrease, the standard mean-field theory for the treatment of electron-electron forces becomes less applicable. Motivated by this fact, effective quantum potentials have been established as a proven way to include quantum-mechanical effects into Monte-Carlo (MC) device simulations. The pseudo-differential operator for the effective quantum potential we build on here is based on a perturbation theory around thermal equilibrium [1, 2], was first derived in [3], and used to include the interaction between potential wells and single electrons in previous work [5, 6].

Other approaches to the inclusion of quantum-mechanical size-quantization effects that have been proposed are an effective potential due to Ferry [7] and the density gradient method [8, 9]. In both there are a number of parameters that do not represent ex-

act physical values, like the size of the electron wavepacket in the effective potential approach and the mass of the carriers in the density gradient methods. An alternative is the direct particle simulation of the dynamics of wave-packets on highly unstructured meshes [10, 11]. The effective quantum potential we use here does not depend on parameters that are hard to estimate and is also generally smoother than the classical potential by two degrees, i.e., two more classical derivatives exist which relieves the problem of statistical noise.

In this work we show that the six-dimensional integral of the pseudo-differential operator formulation of the effective quantum potential can be reduced to a two-dimensional integral that can be readily precomputed and stored. Finally we present 3D MC device simulation results obtained from this formulation.

2. The Effective Quantum Potential for the N -body Problem

The idea of the effective potential approach is to incorporate quantum mechanical corrections into particle based simulators by modifying the classical forces acting on electrons during free flight. Hence the field term $-e\nabla_x V(x)$ in the semi-classical Boltzmann equation

$$\partial_t f + \nabla_x \left(\frac{1}{m_*} p f \right) - \nabla_p (e f \nabla_x V) = Q(f)$$

is replaced by a modified field term $-e\nabla_x V_Q(x, p, \beta)$. Then the trajectories of the electrons are computed by

$$\frac{dx}{dt} = \frac{p}{m_*}, \quad \frac{dp}{dt} = -e\nabla_x V_Q(x, p, \beta),$$

where the time-dependence of the potential is frozen during the free flight phase. $\beta = 1/(KT)$ is the equilibrium temperature. Given a mean field potential $V(x)$ and a particle at x with momentum p , the quantum potential $V_Q(x, p, \beta)$ is given by the PDO

$$\frac{\sinh\left(\frac{\beta\hbar p \cdot \nabla_x}{2im}\right)}{\frac{\beta\hbar p \cdot \nabla_x}{2im}} \exp\left(\frac{\beta\hbar^2}{8m_*} \Delta_x\right)$$

acting on V , i.e.,

$$V_Q(x, p, \beta) = \frac{\sinh\left(\frac{\beta\hbar p \cdot \nabla_x}{2im}\right)}{\frac{\beta\hbar p \cdot \nabla_x}{2im}} \exp\left(\frac{\beta\hbar^2}{8m_*} \Delta_x\right) V(x). \quad (1)$$

This effective quantum potential was derived first in [3].

For the description of particle-particle interactions beyond standard mean field theory we have to extend this approach to an N -body system. After defining the N -dimensional position and momentum vectors $X := (x_1, \dots, x_N)$ and $P := (p_1, \dots, p_N)$, we start from the N -body Wigner and Bloch equations and obtain the N -particle transport equation

$$\partial_t F + \nabla_P E \cdot \nabla_X F - \nabla_X E \cdot \nabla_P F = 0,$$

where F is the N -dimensional Wigner function and E the effective energy. The Coulomb potential is given by

$$G(X) = \frac{1}{N-1} \sum_{j=2}^N \sum_{k=1}^{j-1} g(x_j - x_k), \quad \Delta_x g = \delta(x). \quad (2)$$

Following the same procedure as in the derivation of (1), we arrive at the N -particle effective energy

$$E = \frac{\|P\|^2}{2m_*} + V_Q(X, P, \beta)$$

and the quantum potential

$$V_Q(X, P, \beta) = \frac{\sinh\left(\frac{\beta\hbar P \cdot \nabla_X}{2im}\right)}{\frac{\beta\hbar P \cdot \nabla_X}{2im}} \exp\left(\frac{\beta\hbar^2}{8m_*} \Delta_X\right) G(x).$$

Now the goal is to compute the force acting on one particle, say the one at x_1 . Hence we need $\nabla_{x_1} V_Q(X, P, \beta)$, which is given in the following proposition.

Proposition. *The quantum force $\nabla_{x_1} V_Q(X, P, \beta)$ acting on the particle at x_1 is given by*

$$V_Q(X, P, \beta) = \frac{1}{N-1} \sum_{j=2}^N W(x_1 - x_j, p_1 - p_j),$$

$$W(x, p) := \frac{\sinh\left(\frac{\beta\hbar p \cdot \nabla_x}{2im}\right)}{\frac{\beta\hbar p \cdot \nabla_x}{2im}} \exp\left(\frac{\beta\hbar^2}{4m_*} \Delta_x\right) g(x),$$

where g is the Green function.

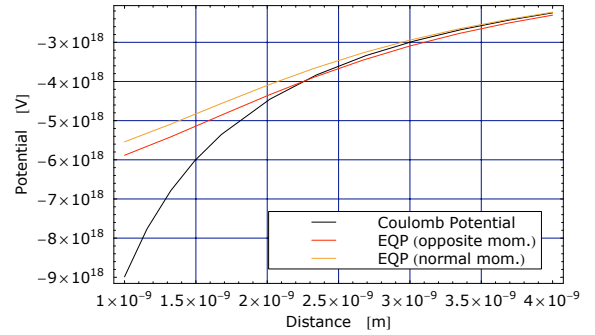


Figure 1: The effective quantum potential (EQP) compared the Coulomb potential. For the EQP the momentum vectors are $(p, 0, 0)$ and $(-p, 0, 0)$ for the opposite momentum curve and $(p, 0, 0)$ and $(0, p, 0)$ for the normal momentum case where $p := 5.40275 \cdot 10^{-26}$.

The six-dimensional integral of the PDO can be reduced to a two-dimensional integral. These integrals can be tabulated as a function of three variables for use in a three-dimensional particle-based Monte Carlo semiconductor device simulator.

For numerical work it is advantageous, if not indispensable, to scale the integration variable. With

the scaling variables ρ the effective quantum potential reads

$$\begin{aligned}
 V_Q((x, \bar{x}), (p, \bar{p}), \beta) &= V_Q(\|x - \bar{x}\|, \|p - \bar{p}\|, \theta, \beta) \\
 &= -\frac{\rho}{8\pi^2\epsilon_0} \int_0^\infty \int_0^{2\pi} \frac{\sinh\left(\frac{\beta\hbar}{2m}\|q\|\rho r \cos\varphi\right)}{\frac{\beta\hbar}{2m}\|q\|\rho r \cos\varphi} \\
 &\cdot \cos(\|y\|\rho r \cos(\varphi - \theta)) \operatorname{erfc}\left(\sqrt{\frac{\beta\hbar^2}{4m_*}}\rho r\right) d\varphi dr.
 \end{aligned}$$

In the special case $p = \bar{p}$ the potential simplifies to

$$-\frac{1}{4\pi\epsilon_0} \frac{1}{\|x - \bar{x}\|} \operatorname{erf}\left(\frac{\|x - \bar{x}\|}{\sqrt{\frac{\beta}{m_*}}\hbar}\right).$$

For the classical limit we find, as expected,

$$\lim_{\hbar \rightarrow 0} V_Q((x, \bar{x}), \beta) = -\frac{1}{4\pi\epsilon_0} \frac{1}{\|x - \bar{x}\|}.$$

3. Simulation Results and Discussion

The effective quantum potential is shown in Figure 1. The SOI device used here (Figure 2) has the following specifications: gate length is 10nm, the source/drain length is 15nm each, the thickness of the silicon on insulator (SOI) layer is 7nm, with p-region width of 10nm makes it a fully-depleted device under normal operating conditions, the gate oxide thickness is 0.8nm, the box oxide thickness is 140nm, the channel doping is uniform at $1.45 \cdot 10^{10}\text{cm}^{-3}$ (intrinsic/undoped), the doping of the source/drain regions equals $5 \cdot 10^{19}\text{cm}^{-3}$, and the gate is assumed to be a metal gate with a work-function adjusted to 4.188. The device is designed in order to achieve the ITRS performance specifications for the year 2016.

The distribution function (Figure 3) shows that inclusion of quantum potential leads to an increase of the high energy tail of the electron distributions at the transition from channel to drain.

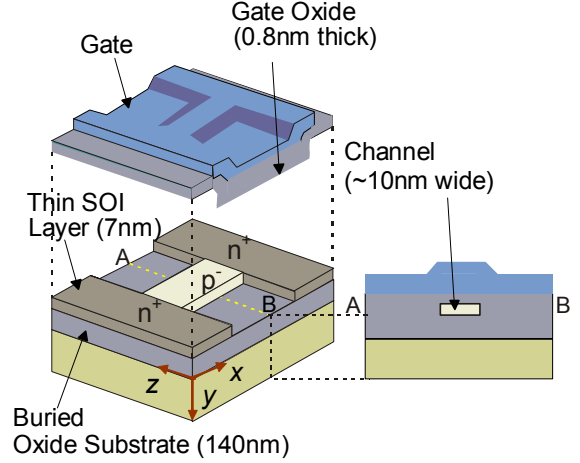


Figure 2: The structure of the simulated 3D device.

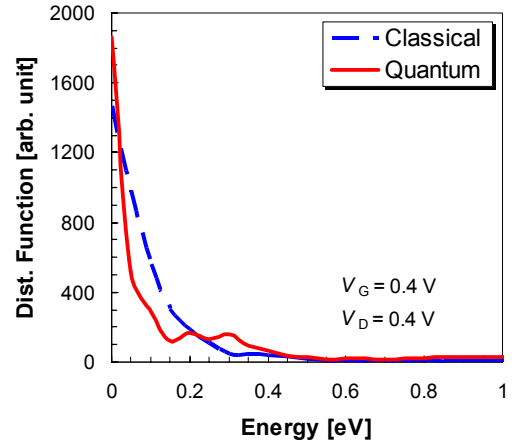


Figure 3: Distribution function.

The simulated output characteristics are shown in Figure 4 with an applied gate bias of 0.4V. Noticeable is the reduced short-channel effects even with an extremely low channel doping density. Inclusion of quantum potential significantly reduces the drive current and transconductance and increases the device threshold voltage as observed from the slope of the linear region. One can also see that the impact of quantization effects reduces as the drain voltage increases (increase in energy) because of the growing bulk nature of the channel electrons.

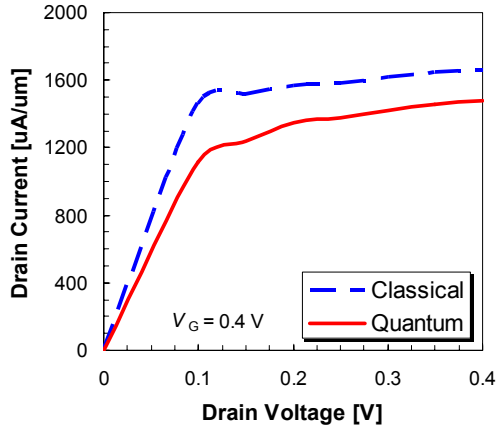


Figure 4: Current-voltage characteristics for a gate bias of 0.4V.

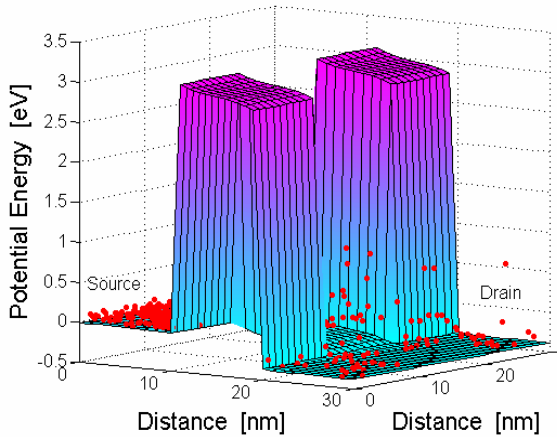


Figure 5: The electron distribution in the device during the simulation.

4. Conclusion

We showed the applicability of a novel effective quantum potential for the N -body problem to 3D MC de-

vice simulations. This method does not use any fitting parameters. The inclusion of particle-particle interactions, as opposed to the classical Coulomb potential, shows a notable difference in the current-voltage characteristics.

Acknowledgment

The authors acknowledge support by the Austrian Science Fund (Fonds zur Förderung der wissenschaftlichen Forschung, FWF) and through National Science Foundation grant DECS-0218008.

References

1. I. Gasser and A. Jünger, "The quantum hydrodynamic model for semiconductors in thermal equilibrium," *Z. Angew. Math. Phys.* **48**, 45 (1997).
2. C. Gardner and C. Ringhofer, "Smooth quantum potential for the hydrodynamic model," *Physical Review* **E53**, 157 (1996).
3. C. Ringhofer *et al.*, "Effective potentials and quantum fluid models: a thermodynamic approach," *Inter. J. on High Speed Electronics and Systems* **13**(3), 771 (2003).
4. C. Heitzinger and C. Ringhofer, "An effective quantum potential for particle-particle interactions in three-dimensional semiconductor device simulations," *Journal of Computational Electronics* (2006), (Submitted for publication).
5. S. Ahmed *et al.*, "Quantum potential approach to modeling nanoscale MOSFETs," *Journal of Computational Electronics* **4**(1-2), 57 (2005).
6. D. Vasileska *et al.*, "Quantum and Coulomb effects in nanodevices," *International Journal of Nanoscience* **4**(3), 305 (2005).
7. D. Ferry, "The onset of quantization in ultra-submicron semiconductor devices," *Superlattices & Microstructures* **27**, 61 (2000).
8. D. Ferry and H. Grubin, "Modelling of quantum transport in semiconductor devices," *Solid State Phys.* **49**, 283 (1995).
9. G. Iafrate *et al.*, "Utilization of quantum distribution functions for ultra-submicron device transport," *Journal de Physique* **42**(Colloque C7), 307 (1981).
10. R. Wyatt, "Quantum wavepacket dynamics with trajectories: Wavefunction synthesis along quantum paths," *Chem. Phys. Lett.* **313**, 189 (1999).
11. R. Wyatt, "Quantum wave packet dynamics with trajectories: Application to reactive scattering," *J. Chem. Phys.* **111**, 4406 (1999).